

A Time-Domain Virtual Electromagnetics Laboratory for Microwave Engineering Education

Wolfgang J. R. Hoefer, *Fellow, IEEE*, and Poman P. M. So, *Senior Member, IEEE*

Abstract—Electrical-engineering students look upon electromagnetic-field theory as a difficult, abstract, and highly mathematical subject. The use of computer modeling and simulation is helpful in making the subject matter more accessible to students in electromagnetics and microwaves courses. In this paper, a complimentary two-dimensional time-domain field simulation software tool (MEFiSTo-2D Classic) is used to illustrate fundamental electromagnetic concepts that are traditionally described by mathematical formulas. The user-friendly interactive features and field animation capabilities of this software transform abstract electromagnetic-field theory into realistic images on the screen. Once the fundamental modeling concepts have been comprehended, students can create advanced structures to explore the subject matter further.

Index Terms—Education, electromagnetic simulation, time-domain modeling, transmission lines, Virtual Electromagnetics Laboratory (VEL), visualization, waveguides.

I. INTRODUCTION

IN THIS PAPER, a series of virtual electromagnetics experiments will be presented in the order of increasing geometrical structure and field complexity. Simple transmission-line structures that support the TEM mode of propagation will be examined. Inhomogeneous medium will then be introduced into the structures to illustrate the concepts of boundary conditions, as well as reflection and transmission at dielectric interfaces. Discontinuities created by junctions, irises, and dielectric objects will be used to demonstrate diffraction, evanescent field behavior, and scattering parameters. Finally, advanced examples such as a branch-line coupler and microwave components containing nonlinear elements will be modeled. Length restrictions do not allow for a detailed description of the numerical method and the implementation of advanced features, such as wide-band absorbing boundaries and nonlinear elements. However, both the compact disc that contains the electronic version of this paper and the install image of the electromagnetic simulator MEFiSTo-2D Classic include the file *2D_Theory.pdf* with a detailed description of the theory of 2D TLM modeling of fields and waves.¹

Manuscript received February 28, 2002. This work was supported in part by the Natural Sciences and Engineering Research Council of Canada, by the Science Council of British Columbia, and by the National Research Council of Canada.

The authors are with the Department of Electrical and Computer Engineering, University of Victoria, Victoria, BC, Canada V8W 3P6 (e-mail: whoef@ece.uvic.ca; poman@ece.uvic.ca).

Digital Object Identifier 10.1109/TMTT.2003.809189

¹This paper has supplementary downloadable material available at <http://ieeexplore.ieee.org>, provided by the authors. This multimedia dataset includes an electronic version of this paper in PDF format. It contains hyperlinks to all other files in this dataset. This material is 19.5 MB in size.

In addition to studying the electromagnetic behavior of structures, this paper also focuses on the use of virtual experimentation software as a versatile and effective teaching/learning tool in both the demonstration and laboratory scenarios. Virtual experimentation is different from replaying a recorded experiment or using a professional computer-aided design (CAD) tool. The former rarely allows intervention—it runs by itself; the latter is usually designed to get output data from specifications rather than providing insight into the process that is being studied or the manner in which the data are generated. The main characteristics of virtual experimentation are full-user interactivity and dynamic visualization of data. Such characteristics are most naturally achieved by time-domain solvers for the following reasons.

- The computer simulation emulates the physical process as it actually occurs in space and time.
- Time-domain virtual experiments resemble real laboratory experiments.
- Causes and effects can be clearly distinguished.
- Both transient and time-harmonic phenomena can be modeled, and a single transient simulation can cover a wide bandwidth.

Note that the simulator MEFiSTo-2D Classic runs only on IBM and compatible computers under Windows 95 (SR2), 98, 2000, ME, XP, or NT version 4.0. For readers using other platforms and operating systems, or for those who do not wish to install MEFiSTo-2D Classic for any reason, we have included a set of animated Gif files that can be opened and run in a web browser. These files reside in the folder *Gif* within the directory that contains the electronic version of this paper.

II. TUTORIAL ON MEFiSTo

In this section, we use a simple uniform plane-wave example to introduce MEFiSTo-2D Classic to readers unfamiliar with time-domain field simulators. However, this tutorial is not meant to replace MEFiSTo's Tutorials and User Manual. Please install MEFiSTo-2D Classic and have its documentation ready for reference (see the Help menu of MEFiSTo for .html documentation, and Start/Programs/MEFiSTo-2D Classic/HelpDoc/PDF for printable manuals and the theory of MEFiSTo in pdf format).

Without loss of generality, a uniform *y*-polarized plane wave propagating in the *z*-direction can be written as

$$E_y(z, t) = E_y \cos(\omega t - kz) \quad (1)$$

where E_y , ω , and k are the magnitude, frequency, and wavenumber, respectively. The equation simply states that, at

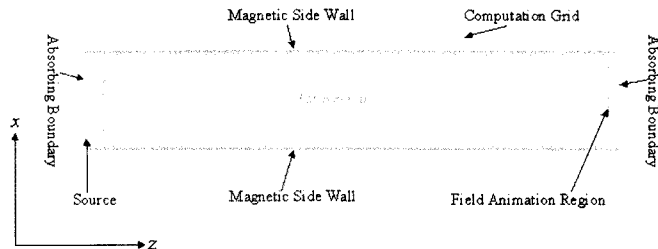


Fig. 1. MEFiSTo drawing for modeling (1). The computational grid has a 1-mm resolution and the source is a 10-GHz sine wave. See the file [01-TEM.tlm](#) for more details regarding excitation and output settings.

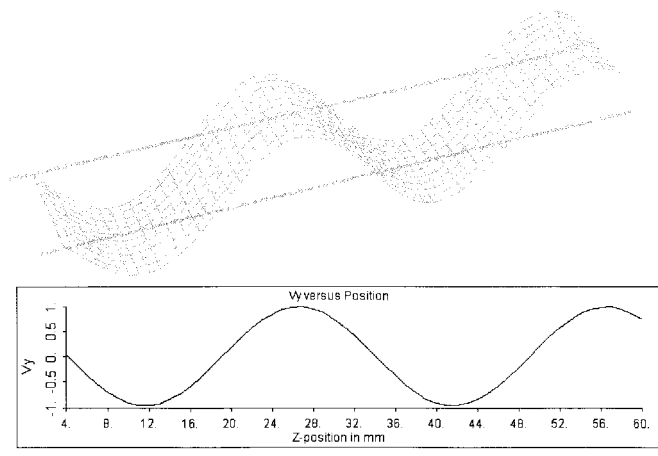


Fig. 2. 10-GHz sine wave is injected from the left-hand side of the structure. The 3-D image indicates that the field is uniform along the x -direction. The graph at the bottom shows that the wavelength is 30 mm.

a fixed point in space, the magnitude of the electric field varies sinusoidally in time. Furthermore, it also implicitly states the wavelength and velocity of propagation, which are $\lambda = 2\pi/k$ and $c = \omega/k$, respectively. The above information can be easily obtained using MEFiSTo-2D Classic; henceforth, it will simply be called MEFiSTo.

Fig. 1 depicts a MEFiSTo drawing for modeling (1). It is a two-dimensional (2-D) computational mesh with magnetic sidewalls. The source at the left-hand side of the structure excites a y -polarized 10-GHz TEM plane wave traveling in the positive z -direction. Fig. 2 shows two screen images from MEFiSTo—the three-dimensional (3-D) field image confirms that the field is uniform along the x -direction; the line graph indicates that the wavelength is indeed 30 mm. Once the wavelength is obtained, other quantities such as the wavenumber and speed of propagation can be computed easily with analytical expressions. MEFiSTo also yields the propagation delay between two points of interest that allows you to compute the speed of propagation based on the separation between them. If you have not yet installed MEFiSTo, please do so now, load the [01-TEM.TLM](#) data file, and start the simulation by clicking on the “++” button. The field animation feature of MEFiSTo allows you to visualize the field moving smoothly in the z -direction. This lifelike animation reveals the dynamic behavior of the time-varying electromagnetic fields described by mathematical formulas such as (1). Note that the slight field distortions at the front of the sine wave are due to numerical

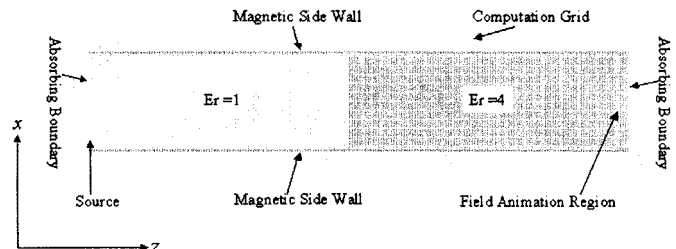


Fig. 3. Half of the air space has been replaced with a dielectric ($Er = 4$). The air–dielectric interface has reflection and transmission coefficients of $-1/3$ and $2/3$, respectively. See any microwave textbook for the theory.

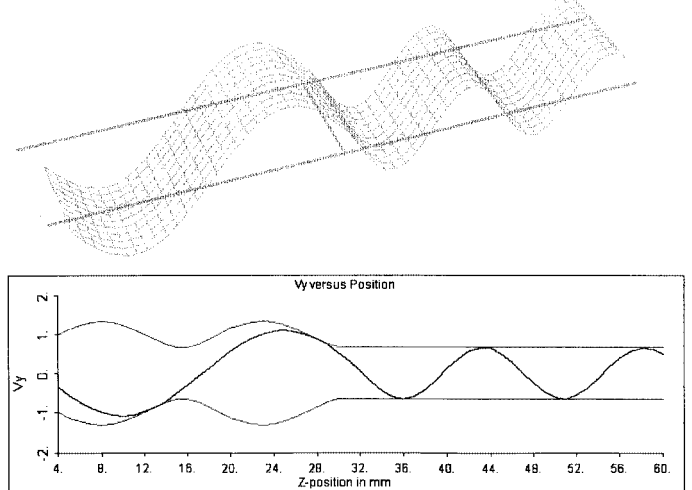


Fig. 4. Snapshots of a 10-GHz sine wave in a mixed air–dielectric medium. The formation of a standing wave, continuity of electric field, as well as partial reflection and transmission at the air–dielectric interface can be seen clearly.

dispersion that affects all space- and time-discrete numerical methods such as finite difference time domain (FDTD) [1], [2] and transmission-line matrix (TLM) [3]–[5].

NOTE: If you use a computer with an operating system other than Windows, you can still run all experiments as animated gif files in your internet browser by clicking on the [gif link](#) and selecting a link with the same name as the corresponding TLM data file.

Now let us replace half of the air region with dielectric of relative permittivity $Er = 4$. The modified drawing is shown in Fig. 3. The dielectric interface at $z = 30$ mm enforces a boundary condition with reflection and transmission coefficients equal to $-1/3$ and $2/3$, respectively. Snapshots of the field are shown in Fig. 4. The modeling setup for this example is stored in the [02-Interface.TLM](#) data file, as well as in an [animated gif](#) of the same name. Interesting dynamic field behavior such as the formation of a standing wave, reflection, and transmission can be observed with MEFiSTo. Since the above examples contain only simple structures in a very small mesh for modern computers, you may find that the simulations run too fast for you to observe the field evolution. If this is the case, you can set MEFiSTo to run in a slow-motion mode by introducing a delay in the control-data dialog box under the simulation-control menu command. Alternatively, you may want to step through the simulation manually by using the “+” button in the simulation toolbar.

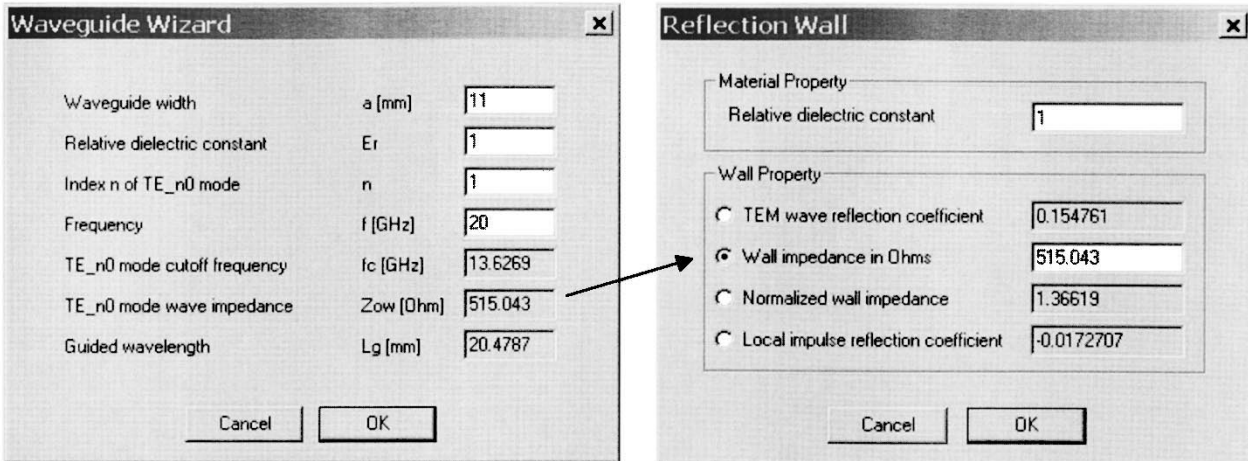


Fig. 5. Screen image of MEFiSTo's waveguide wizard and reflection wall dialog boxes. They are useful when modeling narrow-band absorbing boundaries for TE₁₀-mode operation.

As a last modification before entering the description of the Virtual Electromagnetics Laboratory (VEL), we replace the magnetic sidewalls of the structure in Fig. 1 with electric sidewalls to create a rectangular waveguide. The waveguide wizard shown in Fig. 5 will be helpful in determining the required parameters. The modified structure, shown in Fig. 6, represents the rectangular waveguide. Now we face a challenging problem for time-domain modeling—the dominant mode of propagation is the TE₁₀ mode, and its wave impedance is frequency dependent (dispersive) as follows:

$$Z_w = \frac{120\pi}{\sqrt{1 - (f_c/f)^2}} \quad f_c = \frac{1}{2a\sqrt{\mu\epsilon}} \quad (2)$$

where a is the waveguide width. This, in turn, affects the reflection coefficient of the absorbing boundary that terminates the waveguide. MEFiSTo has a built-in wizard to compute the above quantities. Simply enter the appropriate numbers in the waveguide wizard and transfer the impedance value to the reflection wall dialog box, as shown in Fig. 5.

Fig. 6 depicts snapshots of a 20-GHz wave propagating down the waveguide. MEFiSTo not only models propagating fields in waveguides, but also correctly simulates the behavior of fields at frequencies below cutoff. In this case, fields preserve the transverse profile (in the x -direction), but decay exponentially in the longitudinal direction, as shown in Fig. 7.

III. VEL

The VEL is a suite of simulation experiments that elucidate the behavior of electromagnetic fields and the properties of microwave and millimeter-wave components. All experiments are performed using MEFiSTo. Each virtual experiment is set up using a graphics user interface and stored as a data file with a ".tlm" extension. Of course, each structure can be edited to modify the experiment, or entirely new experiments can be created to suit a particular teaching program. Here is a list of typical virtual electromagnetics experiments for a fundamental course in transmission lines and microwave circuits. The theoretical

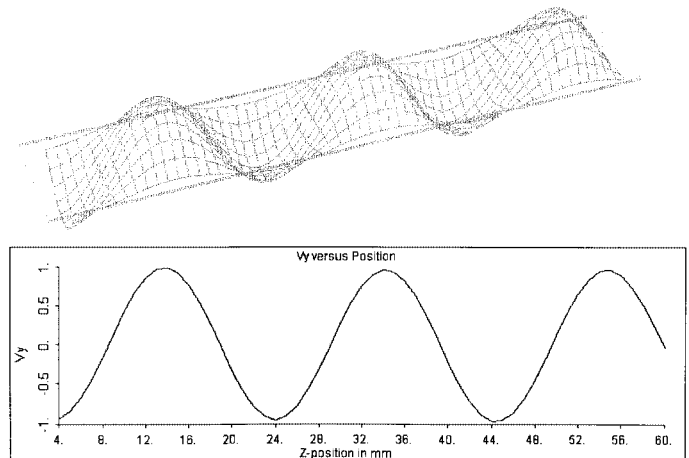


Fig. 6. Rectangular waveguide propagating a TE₁₀ wave at 20 GHz. The V_y versus z -position graph shows that the guided wavelength is approximately 20.5 mm; the theoretical value is 20.4787 mm. The experimental setup for this example is stored in the 03-TE.tlm data file and can be visualized as animated gif.

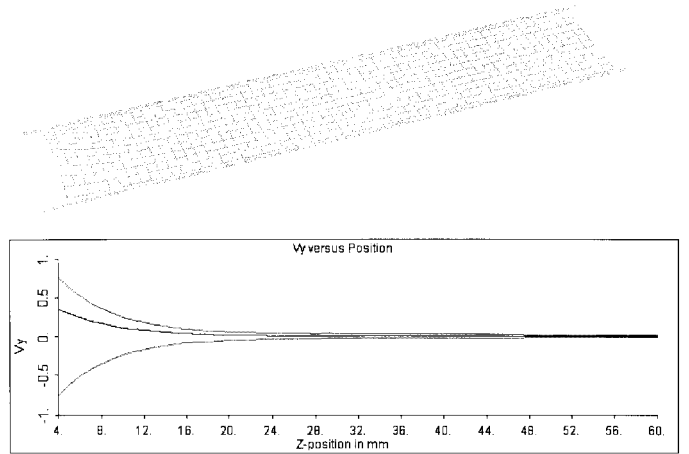


Fig. 7. Same rectangular waveguide is now excited at a frequency below cutoff. The TE₁₀ cutoff frequency is 13.63 GHz. This diagram shows the exponential decay of the fields when a 10-GHz signal is applied at the input port.

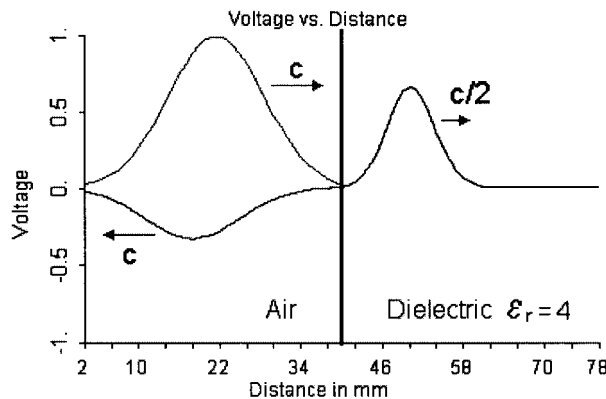


Fig. 8. Scattering of a Gaussian pulse at an air–dielectric discontinuity. The pulse incident from the air with velocity c is scattered at the interface. The dynamic visualization clearly shows the difference in speed and pulselwidth in the two dielectrics, and the continuity of the field at the interface. The simulator emulates a time-domain reflectometer

foundations of these experiments can be found in standard microwave texts and will, thus, not be repeated here. Links to other websites containing detailed lab instructions and MEFiSTo data files can be found at the end of this paper.

Experiment 1: Wave Propagation on TEM Transmission Lines

- A. Propagation along a lossless transmission line.
- B. Propagation of a sine wave.
- C. Reflection of a Gaussian pulse by a short circuit.
- D. Reflection of a Gaussian pulse by an open circuit.
- E. Propagation of a Gaussian pulse.
- F. Partial reflection of a Gaussian pulse by a resistive load.
- G. Reflection of a sine wave by a short circuit.
- H. Reflection of a sine wave by an open circuit.
- I. Partial reflection of a sine wave by a resistive load.
- J. Propagation of a Gaussian pulse on a lossy transmission line.
- K. Propagation of a sine wave along a lossy line.
- L. Scattering of a Gaussian pulse at a dielectric discontinuity.
- M. Scattering of a sine wave at a dielectric discontinuity.
- N. Additional experimentation.

Fig. 8 shows a snapshot of the waves in Experiment 1L. This example demonstrates how the many different aspects of wave scattering can be observed at once in a time-domain simulation, such as the differences in propagation speed in the different media, waveform compression in the dielectric, continuity of voltage across the air–dielectric interface, and the magnitude and phase of the reflected and transmitted waves.

Click on the links above the Figures to view settings, start a MEFiSTo simulation, or select and view an animated gif.

Experiment 2: Wave Propagation in Rectangular Waveguides

The purpose of this experiment is to visualize the field profile of the dominant TE_{10} -mode in rectangular waveguides, and the effects of losses and dispersion of wave velocity and impedance.

- Propagation of a TE_{10} sine wave in a lossless guide

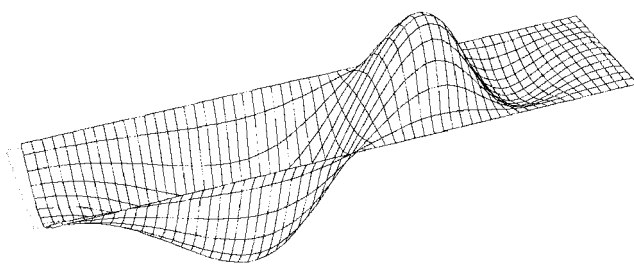


Fig. 9. Response of a rectangular waveguide to a Gaussian excitation clearly demonstrates its dispersive nature and shows the trapping of low-frequency energy at the input side (left-hand side) due to cutoff.

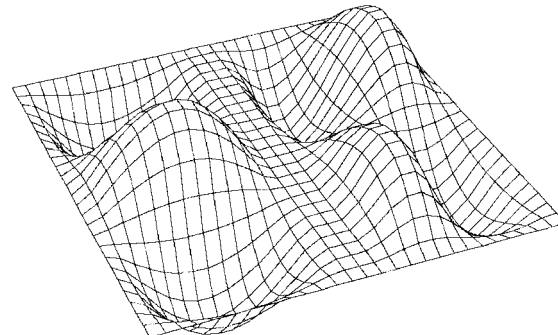


Fig. 10. Dynamic representation of the longitudinal field of the TM_{31} and TM_{22} modes in a rectangular waveguide cross section not only shows the modal field pattern, but also the different cutoff frequencies.

- Reflection of TE_{10} sine waves by short and open circuits
- Reflection of TE_{10} sine waves by a resistive load
- Excitation of a rectangular waveguide by a Gaussian
- Propagation of a TE_{10} sine wave in a lossy waveguide

Fig. 9 demonstrated the dispersive effect of rectangular waveguide on a Gaussian pulse.

Experiment 3: Simulation of Mode Fields in Rectangular Waveguides

- TE_{10} and TE_{20} modes
- TM_{31} and TM_{22} modes

At cutoff, the electric- and magnetic-field components in a rectangular waveguide are independent of the longitudinal coordinate and, thus, form a 2-D resonant problem that can be modeled by MEFiSTo-2D Classic. Since the modal field distributions are sine and cosine functions in the transverse plane, each mode can be excited separately by imposing an appropriate field template in the cross-sectional plane. Fig. 10 depicts the TM_{31} and TM_{22} modes of resonance.

Experiment 4: Scattering at a Discontinuity in a Rectangular Waveguide

- Scattering parameters of an inductive iris
- Field behavior at the discontinuity

In this particular example, the discontinuity acts like an inductance that is connected in shunt across the waveguide. A wide-band transient signal (Gaussian pulse) followed by a discrete Fourier transform of the response yields the S -parameters, Fig. 11, of the discontinuity in a single simulation run.

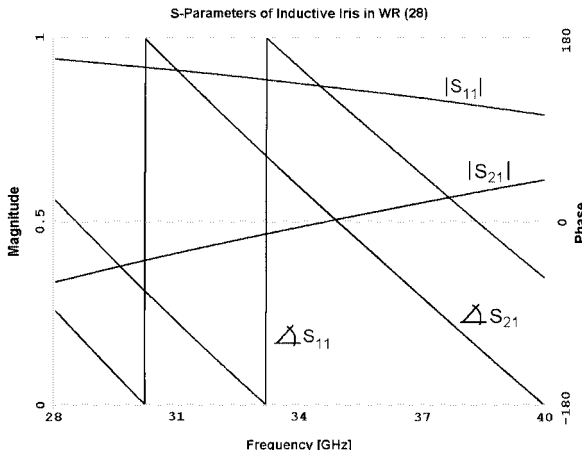


Fig. 11. S -parameter extraction from the Fourier transform of the transient response emulates the functionality of a vector network analyzer.

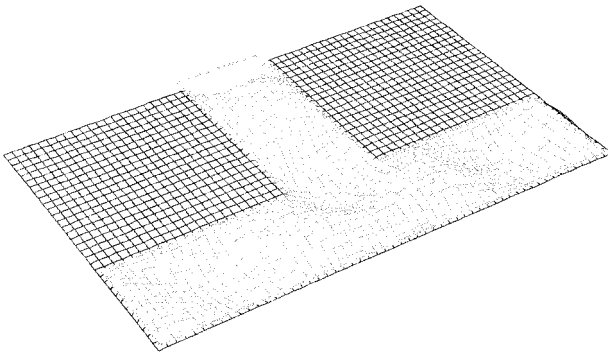


Fig. 12. Experimenting with simple waveguide junctions allows students to observe and to understand the connection between field behavior and S -parameters. The geometry can easily be modified and the resulting effects observed instantly.

Experiment 5: Scattering at a Waveguide T-Junction

- Scattering parameters of the T-junction
- Field behavior at the T-junction

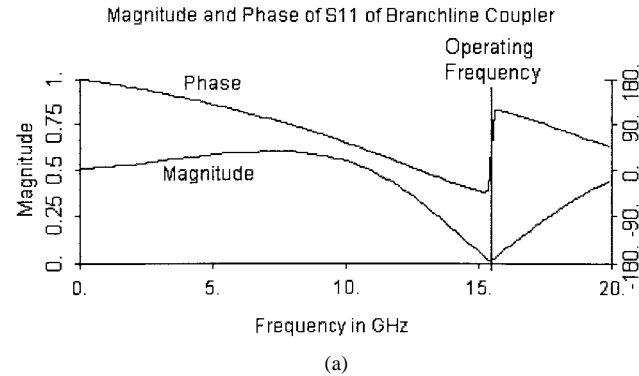
This hybrid junction, shown in Fig. 12, is excited at the basis of the T. Clearly, the junction is not matched, even though the two other ports are both terminated in a matched load.

Experiment 6: Study of a Hybrid Branch-Line Coupler

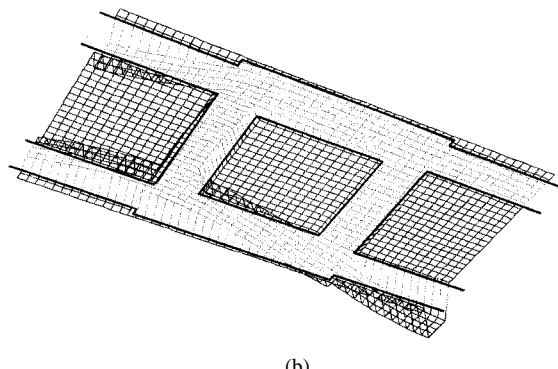
- Scattering parameters of the branch-line coupler
- Field behavior in the branch-line coupler

The characteristics of this important microwave component are easily studied by first performing a wide-band S -parameter analysis and identifying its characteristic operating frequency, Fig. 13(a). A subsequent visualization of the field behavior under time-harmonic excitation clearly shows how it works, Fig. 13(b). The student can then experiment with different terminations of the ports and with different excitation frequencies.

We can now excite one or several ports of the coupler with a sinusoidal signal at the operating frequency determined in Fig. 13(a) and observe the behavior of the field in the component.



(a)



(b)

Fig. 13. (a) Magnitude and phase of S_{11} of a branch-line coupler. The operating frequency of this parallel-plate waveguide model is 15.4 GHz. (b) Snapshot of the field distribution at 15.4 GHz when the port at the upper right-hand side is excited with a sinusoidal signal. The power splitting and phase shift between the two coupled ports are clearly visible in the dynamic visualization. All four ports are matched in this situation.

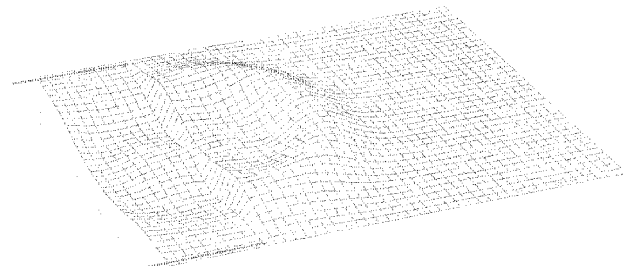


Fig. 14. Small aperture in an absorbing boundary—a fundamental experiment in wave diffraction.

Experiment 7: Diffraction of a Plane Wave by a Small Aperture in an Absorbing Boundary

Fig. 14 depicts a plane wave incident on a small aperture in an absorbing boundary. A circular wavefront emerges on the other side of the aperture.

The following examples are basic diffraction experiments.

Experiment 8: Diffraction of a Plane Wave by a Knife Edge

Fig. 15 shows a plane wave incident on a conducting knife-edge. Part of the wave moves forward and is diffracted around the edge, while the other part is reflected and travels backwards.



Fig. 15. Diffraction of a Gaussian at a conducting knife-edge—another fundamental experiment in wave diffraction.



Fig. 16. Complex field pattern observed in these scattering experiments is the result of internal resonances in a dielectric cylinder of square cross section. The cylinder rings for a long time after the incidence of a Gaussian pulse and radiates energy in all directions until its internal resonances have decayed.

Experiment 9: Scattering of a Plane Wave by a Dielectric Cylinder of Square Cross Section

- Scattering of a wave with polarization parallel to the cylinder axis
- Scattering of a wave with polarization perpendicular to the cylinder axis

Fig. 16 depicts the complex field created by the incidence of a plane wave on a dielectric cylinder. Two different scenarios can be modeled.

Experiment 10: Scattering of a Plane Wave by a Helicopter

While this experiment does not represent the truly 3-D scattering by a real helicopter, the two-dimensional model shown in Fig. 17 nevertheless demonstrates what happens when a plane-wave pulse hits a complex reflecting object. The magnetic sidewalls orthogonal to the wavefront preserve the incident wave shape, but reflect the scattered field back toward the helicopter.

Experiment 11: Parametric Frequency Halving Using Varactor Diodes

- Visualization of the frequency-halving process
- Visualization of the field behavior in the halver

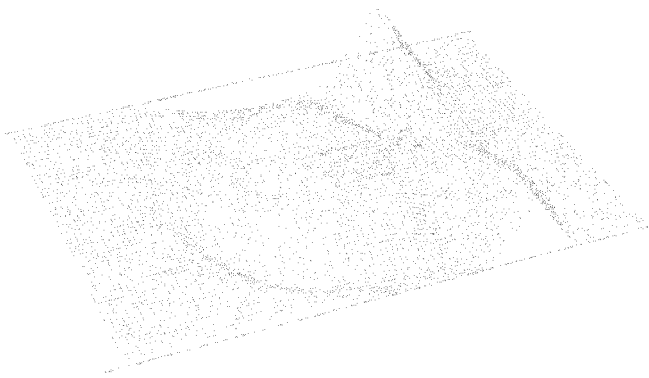
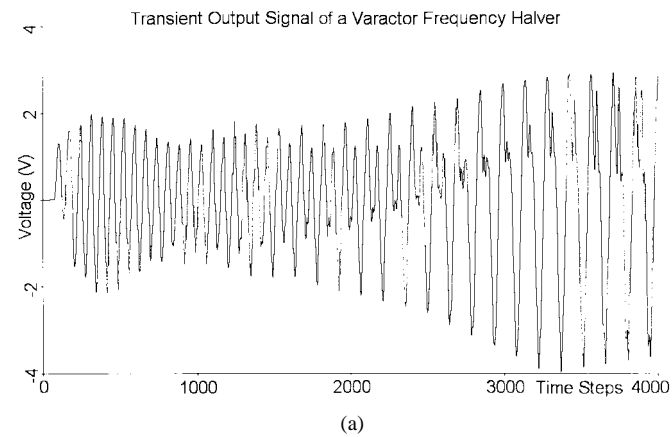
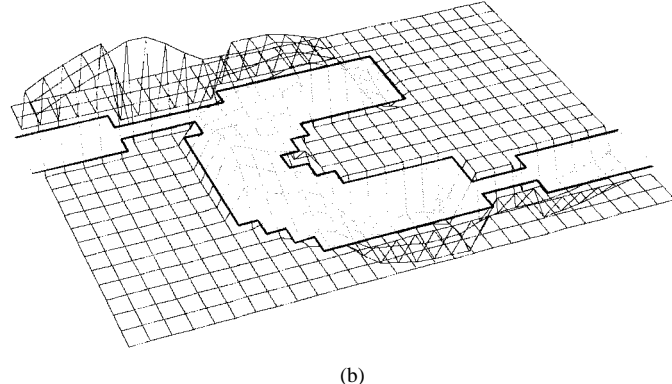


Fig. 17. Scattering of an electromagnetic pulse by an object of complex geometry is demonstrated in this example. By analyzing the signal reflected by the object, the student can investigate the features of its electromagnetic signature, such as delays in the signal components reflected from various parts, and characteristic resonances.



(a)



(b)

Fig. 18. (a) Output signal of a varactor frequency halver shows the progressive transfer of energy from the 12-GHz excitation signal to the 6-GHz subharmonic. (b) Layout and field distribution in the varactor halver after 9000 time steps. The 12-GHz signal enters from the top left-hand side.

In this interesting application, two varactor diodes are placed in the extremities of a horseshoe resonator [6], [7]². At 6 GHz, the structure resonates with the extremities out-of-phase, while at 12 GHz, they are in-phase. The nonlinear capacitance of the varactors transfers energy from the 12 GHz to the 6-GHz mode of resonance, Fig. 18.

²The content of this book is also included in pdf format in the install image of MEFiSTo-2D Classic under the file name “2D_Theory.pdf.”

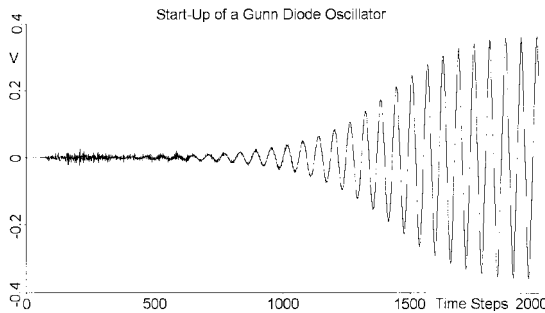


Fig. 19. Modeling of the start-up of a Gunn diode oscillator. A nonlinear device is embedded into the field model [8]. Noise is injected, and the device begins to selectively amplify the natural resonant frequencies of the oscillator circuit. One time step corresponds to 0.578 ps. The oscillator generates output at 28 GHz.

Experiment 12: Microwave Oscillator With Negative Conductance (Tunnel or Gunn) Diode

- Visualization of the start of oscillations
- Visualization of the field in the oscillator
- Visualization of the output spectrum of the oscillator

The active diode model of MEFiSTo allows the modeling of oscillators in the time domain. In addition to the startup (see Fig. 19) and spectrum of the oscillator, students can also study the phenomenon of injection locking by means of a small sinusoidal signal injected into the port of the oscillator.

IV. ADDITIONAL MEFiSTo EXPERIMENTS

We highly recommend the following excellent teaching websites that feature teaching applications of MEFiSTo-2D Classic.

- 1) *University of Ulm, Ulm, Germany, Prof. Wolfgang Menzel*: This website contains various animated GIFs created with MEFiSTo-2D Classic, as well as a library of MEFiSTo data files that can be downloaded and run with MEFiSTo-2D Classic. Applications include transmission lines, waveguides, couplers, filters and EMC scenarios. [Online]. Available: <http://mwt.e-technik.uni-ulm.de/world/lehre/hf-anim/mefisto/index.html>
- 2) *McMaster University, Hamilton, ON, Canada, Prof. Natalia Georgieva-Nikolova*: This 25-page document describes in detail the theoretical foundations of TEM transmission lines and ten corresponding MEFiSTo-2D Classic virtual electromagnetic laboratory experiments. [Online]. Available: http://ece.eng.mcmaster.ca/faculty/georgieva/EM_downloads/TEM_lab.pdf
- 3) *University of Queensland, Brisbane, Qld., Australia, Prof. Nicholas Shuley*: This 14-page document features laboratory notes on basic transmission-line experiments and detailed instructions on how to set up these experiments on MEFiSTo-2D Classic. [Online]. Available: <http://www.itee.uq.edu.au/~elec3100/simulation.pdf>

V. SUMMARY AND CONCLUSIONS

The present and future generations of students expect computers to be an integral part of their education and are often

motivated by sophisticated computer tools that complement traditional theory and laboratory material. This is particularly true for abstract and theoretically demanding areas such as microwave engineering. It is thus increasingly attractive for educators to use “virtual experiments” on computers for education, such as the examples presented in this paper. The benefits include: 1) stimulation of interest due to fast simulation speed and quick return of results; 2) familiarization with electromagnetic modeling methods; 3) possibility to test new ideas quickly; 4) deeper physical insight due to visualization and animation of electromagnetic fields; 5) ability to identify dominant and parasitic effects; and 6) ability to “see” and understand the connection between field behavior and electrical characteristics of components or systems. Time-domain simulators provide a realistic modeling environment that evokes the instruments usually found in a microwave laboratory, such as network analyzers, spectrum analyzers, and oscilloscopes. In addition, they allow dynamic visualization of fields, thus revealing the physical mechanisms that cause the electrical characteristics of structures and circuits.

ACKNOWLEDGMENT

The authors would like to thank the Faustus Scientific Corporation, Victoria, BC, Canada ([Online]. Available: <http://www.faustcorp.com>) for providing the complimentary simulation software MEFiSTo-2D Classic and electronic documentation.

The latest install image of MEFiSTo-2D Classic can be downloaded free of charge from the Web site of the Faustus Scientific Corporation. [Online]. Available: <http://www.faustcorp.com/downloads/>.

To install MEFiSTo-2D Classic and its complete documentation directly from the CD that contains this paper in electronic form, go directly to the MEFiSTo install the page located in the CD directory that contains this paper. [Online]. Available: http://www.faustcorp.com/html_documents/mefisto_2d_classic/classic.html.

REFERENCES

- [1] K. S. Yee, “Numerical solution of initial boundary value problems involving Maxwell’s equations in isotropic media,” *IEEE Trans. Antennas Propagat.*, vol. AP-14, pp. 302–307, 1966.
- [2] A. Taflove, *Computational Electrodynamics: The Finite-Difference Time-Domain Method*. Norwood, MA: Artech House, 1995.
- [3] P. B. Johns and R. L. Beurle, “Numerical solution of 2-dimensional scattering problem using a transmission line matrix,” *Proc. Inst. Elect. Eng.*, vol. 118, pp. 1203–1208, Sept. 1971.
- [4] W. J. R. Hoefer, “The transmission line matrix method—Theory and application,” *IEEE Trans. Microwave Theory Tech.*, vol. MTT-33, pp. 882–893, Oct. 1985.
- [5] C. Christopoulos, *The Transmission-Line Modeling Method*. Piscataway, NJ: IEEE Press, 1995.
- [6] P. P. M. So, P. P. M. Eswarappa, and W. J. R. Hoefer, “A two-dimensional TLM microwave field simulator using new concepts and procedures,” *IEEE Trans. Microwave Theory Tech.*, vol. 37, pp. 1877–1884, Dec. 1989.
- [7] W. J. R. Hoefer and P. P. M. So, *The Electromagnetic Wave Field Simulator*. New York: Wiley, 1991.
- [8] P. Russer, P. P. M. So, and W. J. R. Hoefer, “Modeling of nonlinear active regions in TLM,” *IEEE Microwave Guided Wave Lett.*, vol. 1, pp. 10–13, Jan. 1991.



Wolfgang J. R. Hoefer (M'71–SM'78–F'91) received the Dipl.-Ing. degree in electrical engineering from the Technische Hochschule Aachen, Aachen, Germany, in 1965, and the D.Eng. degree from the University of Grenoble, Grenoble, France, in 1968.

From 1968 to 1969, he was a Lecturer with the Institut Universitaire de Technologie de Grenoble, Grenoble, France, and a Research Fellow with the Institut National Polytechnique de Grenoble, Grenoble, France. In 1969, he joined the Department of Electrical Engineering, University of Ottawa, Ottawa, ON, Canada, where he was a Professor until March 1992. Since April 1992, he holds the Natural Sciences and Engineering Research Council (NSERC) Industrial Research Chair in Radio Frequency Engineering with the Department of Electrical and Computer Engineering, University of Victoria, Victoria, BC, Canada. During several sabbatical leaves, he has been a Visiting Scientist and Professor with the Space Division of AEG-Telefunken, Backnang, Germany (now ATN), the Electromagnetics Laboratory, Institut National Polytechnique de Grenoble, the Space Electronics Directorate, Communications Research Centre, Ottawa, ON, Canada, the University of Rome "Tor Vergata," Rome, Italy, the University of Nice–Sophia Antipolis, France, the Technical University of Munich, Munich, Germany, the Ferdinand Braun Institute for High Frequencies, Berlin, Germany, and the Gerhard Mercator University, Duisburg, Germany. In 1989, he was an Invited Lansdowne Lecturer with the University of Victoria. His research interests include numerical techniques for modeling electromagnetic fields and waves, CAD of microwave and millimeter-wave circuits, microwave measurement techniques, and engineering education. He is the cofounder and Managing Editor of the *International Journal of Numerical Modeling*. He serves on the Editorial Boards of the Proceedings of the *Institution of Electrical Engineers*, the *International Journal of Microwave and Millimeter-Wave Computer Aided Engineering, Electromagnetics*, and the *Microwave and Optical Technology Letters*.

Dr. Hoefer is a Fellow of the British Columbia Advanced Systems Institute (BC-ASI). He serves regularly on the Technical Program Committees of the IEEE Microwave Theory and Techniques Society (IEEE MTT-S) and IEEE Antennas and Propagation (IEEE AP-S) Symposia. He is the chair of the IEEE MTT-S Technical Committee on Field Theory (MTT-15). He was an associate editor for the IEEE TRANSACTIONS ON MICROWAVE THEORY AND TECHNIQUES (1998–2000). He was a guest editor of the Symposium Issue of the IEEE TRANSACTIONS ON MICROWAVE THEORY AND TECHNIQUES (December 2002). He serves on the Editorial Board of the IEEE TRANSACTIONS ON MICROWAVE THEORY AND TECHNIQUES. He was the recipient of the 1990 Peter B. Johns Prize for the best paper published in the *International Journal of Numerical Modeling*.



Poman P. M. So (M'87–SM'00) received the B.Sc. degree in computer science and physics from the University of Toronto, Toronto, ON, Canada, in 1985, the B.A.Sc. and M.A.Sc. degrees in electrical engineering from the University of Ottawa, Ottawa, ON, Canada, in 1985 and 1987, respectively, and the Ph.D. degree from the University of Victoria, Victoria, BC, Canada, in 1996.

He is currently an Adjunct Assistant Professor and a Senior Research Engineer with the Department of Electrical and Computer Engineering, University of

Victoria. He possesses over 15 years of hands-on experience in object-oriented software development for microwave and millimeter-wave engineering using the TLM method. From April 1997 to June 1998, he was a Senior Antenna Engineer with EMS Canada Ltd. (formerly Spar Aerospace Ltd.). His research has included high-frequency (10–40 GHz) antennas and feed components design for commercial satellite systems, as well as Ku -band active antenna CAD software development. In October 1993, he was invited to the Ferdinand-Braun-Institut für Hochfrequenztechnik Berlin, Berlin, Germany, as a Research Scientist. From August 1990 to February 1991, he was a Visiting Researcher with the University of Rome, Rome, Italy, and the Laboratoire d'Electronique, Sophia Antipolis, France. During his time abroad, he developed a number of electromagnetic wave simulators for the Digital MPP and Connection Machine CM2 massively parallel computers. He is a co-founder of the Faustus Scientific Corporation, and is the creator and chief software architect of the MEFiSTo line of products of the Faustus Scientific Corporation. He is a reviewer for the *International Journal of Numerical Modeling—Electronic Networks, Devices and Fields*.

Dr. So is a Registered Professional Engineer in the Province of British Columbia, Canada.